Polymer Degradation and Stability 96 (2011) 1919–1926

Contents lists available at ScienceDirect

Polymer Degradation and Stability

journal homepage: www.elsevier.com/locate/polydegstab

Formulation selection of aliphatic aromatic biodegradable polyester film exposed to UV/solar radiation

Thitisilp Kijchavengkul [a], Rafael Auras [a,*], Maria Rubino [a], Susan Selke [a], Mathieu Ngouajio [b], R. Thomas Fernandez [b]

[a] School of Packaging, Packaging Building, Michigan State University, East Lansing, MI 48824 1223, USA
[b] Department of Horticulture, Plant & Soil Science Building, Michigan State University, East Lansing, MI 48824 1223, USA

ARTICLE INFO

Article history:
Received 20 April 2011
Received in revised form
23 June 2011
Accepted 3 July 2011
Available online 13 July 2011

Keywords:
Response surface methodology
Photodegradation
Poly(butylene adipate-co-terephthalate)
PBAT
Biodegradation

ABSTRACT

Aliphatic aromatic copolyester films, poly(butylene adipate-*co*-terephthalate) or PBAT, are susceptible to photodegradation, leading to main chain scission and crosslinking. The presence of crosslinked structures not only decreased the mechanical properties of the film due to embrittlement, but also hindered the biodegradation process by limiting access of water and microorganisms to the polymer chains. This has limited the use of PBAT for outdoor applications, such as mulch films. In this study, response surface methodology (RSM) was used to determine the optimal concentrations of carbon black (CB) and the chain breaking antioxidant butylated hydroxytoluene (BHT) for the design of mulch films that can prevent the formation of crosslinked structures from recombination of free radicals. An overlaid contour plot of suitable concentrations of CB and BHT for the formulation of mulch film for crop production in Michigan or regions with similar solar radiation was established using selection criteria of light transmission of less than 20%, final tensile strength of at least 6.35 MPa, maximum gel fraction of 0.30, and positive number average molecular weight reduction sensitivity in the early stage of degradation.

1. Introduction

In applications where polymer films are used outdoors, such as mulch and greenhouse films, they must endure several types of atmospheric degradation, particularly photodegradation from ultraviolet (UV) exposure. Because of their chemical structure (Fig. 1), aliphatic aromatic biodegradable polyesters, such as poly(butylene adipate-*co*-terephthalate) or PBAT are susceptible to photodegradation, which limits their use, especially outdoors. PBAT presents two different types of photosensitive groups, benzene rings and carbonyl groups. The benzene rings in the aromatic domain can inhibit photodegradation by absorbing UV energy and act as an energy sink by dissipating the UV energy via electron delocalization [1]. However, carbonyl groups in the ester linkages absorb UV radiation energy and cause chain scission via Norrish I and/or Norrish II reactions depending on environmental conditions and polymer structure [2]. High amounts of carbonyl groups present in PBAT make these films susceptible to photodegradation. Furthermore, after the free radicals are formed via Norrish I, the oxidation process is followed by a photooxidation process. As the photooxidation continues, the random main chain scission occurs at more locations. This chain cleavage critically reduces mechanical properties, such as tensile strength, a property necessary to provide soil protection and prevent weed growth [3].

Besides random main chain scission either via Norrish I or Norrish II reactions due to the absorption of UV energy by the carbonyl groups that can negatively affect the performance of the films, crosslinking within the film due to the recombination of free radicals generated from Norrish I [4–6] can reduce its ductility and hence the film becomes more brittle, which is undesirable. Mulch films should be ductile in order to allow the film to stretch, as in the case when winds blow forcing the films to lift from the soil surface. Furthermore, crosslinked structures in the film inhibit the biodegradation process when the polymer film comes into contact with microorganisms, since the crosslinked structures make the film more rigid and also limit access of water and microorganisms to the polymer chains [7].

Since crosslinking in PBAT occurs because of the recombination of free radicals, especially phenyl radicals, a potential solution to radical recombination is to minimize the amount of free radicals that are produced during the photooxidation process. Although there is a substantial amount of the aromatic domain (40–50% mol) in the PBAT structure [8,9] that can dissipate photon energy, antioxidants, such as 2,6-di-tert-butyl-4-methyl phenol or butylated

* Corresponding author. Tel.: +1 517 432 3254; fax: +1 517 353 8999.
E-mail address: aurasraf@msu.edu (R. Auras).

0141-3910/$ – see front matter © 2011 Elsevier Ltd. All rights reserved.
doi:10.1016/j.polymdegradstab.2011.07.001

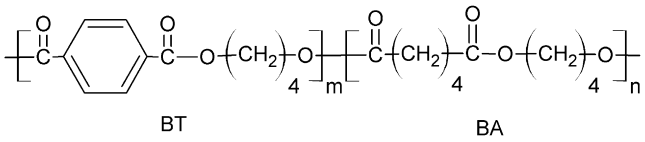

Fig. 1. Structure of poly(butylene adipate-*co*-terephthalate) (PBAT) with aliphatic (BA) and aromatic (BT) domains.

hydroxytoluene (BHT) could be incorporated into the PBAT mulch films to reduce the amount of free radicals produced from UV exposure. The main purposes of adding carbon black (CB) into the mulch film are to block the light transmission in the photosynthetically active radiation (PAR) wavelengths to the soil during the growing season in order to prevent weed growth and to create film with black color to increase soil temperature especially in the root zone [10]. However, CB can also be used to inhibit photodegradation since it can absorb photon energy and reduce the intensity of the light reacting with the polymer [11]. Since there are multiple factors that need to be designed to affect the overall properties of the PBAT mulch films, the objective of this study was to use response surface methodology (RSM) to determine the precise range of concentrations of CB and antioxidants that lead to optimal performance of biodegradable mulch films.

2. Materials and methods

2.1. RSM design of experiment

RSM was used in this experiment because RSM is a methodology that combines both mathematical and statistical techniques in order to develop, improve, or optimize processes, of which multiple input variables and their interactions could affect performance, quality characteristics, or responses of the products or processes [12]. For this experiment, a 2 by 2 factorial rotatable central composite design (CCD) with α of 1.414 was selected. The two selected factors were the concentrations of CB and antioxidant (AnOx). The selected antioxidant for the experiment was BHT, a chain breaking antioxidant. BHT was considered since it is widely used and easily detected by various instruments, such as liquid chromatography or nuclear magnetic resonance (NMR).

Table 1 summarizes actual concentrations in percent by mass, and coded levels of CB and antioxidant matching the rotatable central composite design. There are five different concentrations for each compound coded as −1.414, −1, 0, 1, and 1.414. The coded levels are used in the calculation of the RSM. Since all 12 treatments of film could not be produced in one day, an orthogonal block design was applied. Block 1, consisting of treatments with coded level of −1, 0, and 1, was produced one day, while Block 2, consisting of treatments with coded level of −1.414, 0, and 1.414, was produced another day (Table 1). Trial orders within each block were randomized. In this experiment, the amount of each additive was limited to be at most 1%, which is the limit in the ASTM D6400 compostable specification for additives without requiring further biodegradation and toxicity tests [13]. The center point of 0.39% CB was based on the manufacturing specification of the films used in a preliminary tomato production experiment [3,14,15].

2.2. Film production

For each trial, specific amounts of PBAT with CB master batch (both from Northern Technologies International Inc., Circle Pines, MN) and BHT (Sigma Aldrich, St. Louis, MO) were added to the PBAT resin with 40% mol aromatic (BT) content (BASF, Florham Park, NJ) (Table 1). The master batch contained 10% CB in PBAT resin by mass. Then the mixture was extruded and blown into film using a Killion KLB 100 blown film extruder (Davis-Standard LLC, Pawcatuck, CT) with a screw diameter of 25.4 mm (1 inch), screw length/diameter ratio of 24:1 and a blown die diameter of 50.8 mm (2 inch). The temperature profile of the extrusion process was 177–177–177–170–165–165–165 °C for barrel zone 1, 2, 3, clamp ring, adapter, die 1 and 2, respectively. A screw speed of 21.5 rpm and take up speed of and 0.033 m/s were used. The overall thickness of the produced PBAT films for the 12 treatments was 75.4 ± 10.5 μm (1.9 ± 0.4 mil).

Table 1
Detailed list of all 12 treatments used in the rotatable central composite design (CCD).

Treatment	Block	Actual concentration (% by mass)		Coded level	
		CB	*AnOx*	CB_C	$AnOx_C$
1	1	0.10	0.85	−1	1
2	1	0.39	0.50	0	0
3	1	0.39	0.50	0	0
4	1	0.10	0.15	−1	−1
5	1	0.82	0.85	1	1
6	1	0.82	0.15	1	−1
7	2	0.39	0.50	0	0
8	2	0.39	0.50	0	0
9	2	1.04	0.50	1.414	0
10	2	0.39	1.00	0	1.414
11	2	0.00	0.50	−1.414	0
12	2	0.39	0.00	0	−1.414

Note: The carbon black (CB) concentration levels were coded based on natural log transformation $CB_c = 2\sqrt{2}\ln(CB + e^{-0.5})$, where CB = uncoded concentration of carbon black and CB_C = coded concentration of carbon black. The antioxidant concentration levels were coded based on linear transformation $AnOx_c = \sqrt{2}(2AnOx - 1)$, where $AnOx$ = uncoded concentration of antioxidant and $AnOx_C$ = coded concentration of antioxidant.

2.3. UV simulating cycle (UVSC)

To simulate the three-to-four month use of biodegradable mulch film in Michigan or regions with similar climate from May to September, where the films are exposed to 1500 MJ/m^2 of radiation (average solar radiation 14 MJ/m^2/d) in the laboratory, the PBAT film samples were exposed to UV-A light (long wave UV with wavelength range of 320–400 nm) in the 12-h light/dark cycle for 6 weeks to simulate the exposure the films had during the field exposure. This 12-h light/dark cycle includes an 8-h cycle when the mulch film is exposed to UV light in order to reproduce daylight conditions and a 4-h dark cycle to replicate night conditions. The exposure was carried out in a QUV Accelerated Weathering Tester (Q-Panel Lab, Cleveland, OH) using 8 UVA-340 lamps, which have an irradiance spectrum close to solar radiation. The average irradiance of the preliminary field experiment was 0.70 W/m^2/nm during the photodegradation period, which started once the mulch films were laid in June through harvesting in September in Michigan [3,7]. In the laboratory conditions, an irradiance of 1.40 W/m^2/nm was used to accelerate the simulation [7]. The changes in light transmission and the molecular weight, gel fraction, and mechanical properties of the film as a function of time were determined.

2.4. Light transmission

Percentage of light transmission of the films in the PAR region was determined using a Lambda 25 UV/Visible spectrophotometer from PerkinElmer with an integrating sphere (Wellesley, MA). For each film, three samples were scanned from wavelength 400–700 nm [15]. Average percentage of light transmission was

calculated from the integrated area under the light transmission spectrum divided by the bandwidth of 300 nm.

2.5. Mechanical properties

A universal tester machine from Instron, Inc. (Norwood, MA) was used to test tensile strength, percentage of elongation, and tensile modulus on three samples for each film in the machine direction (MD). Although ASTM D 882 standard requires that at least five samples should be tested, only three samples were tested in this study due to the limitation of the size of the sample holder in the UV chamber. In accordance with the standard, the initial grip length was set at 1 inch (2.5 cm), and grip separation rates of 0.1 or 10 inch/min (0.25 or 25 cm/min) were used depending on the initial strain of the sample [16].

2.6. Molecular weight

The number average molecular weight (M_n) of the samples was determined by dissolving the PBAT sample in HPLC grade tetrahydrofuran (THF), from Pharmco-Aaper (Brookfield, CT), at a concentration of 2 mg/mL. After dissolution, the sample was filtered through a 0.45 μm polytetrafluoroethylene syringe filter. One hundred μL of sample solution was injected into a gel permeation chromatograph equipped with three 7.8 mm × 300 mm 5 μm single pore styrene divinylbenzene particle columns and a refractive index detector (Waters®, Milford, MA) using a flow rate of 1 mL/min, a runtime of 45 min, and a column temperature of 35 °C. A third-order polynomial calibration curve was constructed using polystyrene standards with ten different molecular weights (ranging from 1.20×10^3 to 3.64×10^6 g/mol).

2.7. Gel fraction measurement

Gel fraction is the ratio or the percentage by mass of insoluble polymer in a specified solvent after extraction [17]. Gel fraction is dimensionless, and throughout the paper, the unit of gel fraction is defined as mg/mg, which refers to fraction of insoluble polymer (gel) mass in mg in total polymer mass in mg. The gel fraction of the film samples was measured according to ASTM D 2765 using THF as the solvent [17]. The detailed methodology can be found in Kijchavengkul et al. [18].

2.8. Data analysis

The changes of light transmission, M_n, gel fraction, and tensile strength were plotted for all treatments as a function of total UV radiation, which is linearly proportional to the sample exposure time. The values obtained from various properties such as light transmission, gel fraction, and mechanical properties of the UV exposed films were used as dependent variables for fitting multiple response surfaces, while the coded levels of CB and AnOx concentrations were used as independent variables.

Then a second-order response surface with interaction and blocking effects

$$E\{Y\} = \beta_0 + \beta_1 CB_c + \beta_2 AnOx_c + \beta_{11} CB_c^2 + \beta_{22} AnOx_c^2 + \beta_{12} CB_c \times AnOx_c + \tau(\text{block}) \quad (1)$$

was assigned to a particular parameter using JMP 8.0 software (SAS Institute Inc., Cary, NC). Generally, a second-order response surface equation is sufficient to represent experimental data such as that obtained in this study. With this model (Equation (1)), the investigated responses $E\{Y\}$'s such as light transmission, mechanical properties, gel fraction or molecular weight, are a function of the coded level of CB (CB_C) and antioxidant ($AnOx_C$) as defined by an intercept (β_0), linear main effects of CB (β_1) and antioxidant (β_2), quadratic main effect of CB (β_{11}) and antioxidant (β_{22}), an interaction of CB and antioxidant (β_{12}), and blocking effect (τ).

3. Results and discussion

3.1. Light transmission

Since light transmission, especially the ability of the film to block light in the PAR wavelength, is more important during the early part of the growing season and there were few changes in the film light transmission, the initial values of % light transmission of all 12 treatments were used in the second-order RSM model (Table 2). In the treatments with high % light transmission or carbon black concentration of 0.1% or lower, such as treatments 1, 4, and 11, the variation of the film thickness may increase the variation in the % light transmission (S.D. > 3% transmission). The ANOVA (Table 3) indicates that the second-order RSM model is applicable to the initial light transmission experimental data with R^2 of 0.9906 and p-value of <0.0001.

Also, from the parameter estimates (Table 4), both linear and quadratic main effects of the coded level of CB affected the % light transmission of the PBAT samples with p-value <0.0001. The negative estimated parameter for CB_C indicates as expected that increased concentration of CB will decrease the % light transmission. On the other hand, antioxidant concentration did not play any important role in % light transmission with p-value of 0.5150.

3.2. Tensile strength

Tensile strength of the 12 treatments of PBAT films before the UV exposure was not different. However, during the 6 weeks of UV exposure, the tensile strength of all the treatments decreased exponentially from 19.82–26.81 MPa to 4.00–7.91 MPa following a first order exponential reduction (Fig. 2). As a result, a non-linear first order reduction

$$TS = TS_o + TS_a e^{-TS_b x} \quad (2)$$

was used to fit to the tensile strength reduction pattern. The fitted parameters and the R^2 value are reported in Table 5. The estimated tensile strength of PBAT exposed to x MJ/m^2 of UV radiation (TS) is a function of three parameters: estimated final tensile strength (TS_o), total amount of tensile strength reduction from the beginning to the end of the exposure (TS_a), and reduction rate (TS_b). The non-linear first order reduction equation describes well the reduction of tensile strength from UV exposure, since the R^2 values of all the treatments were 0.89 or greater.

Table 2
Initial light transmission (%) of all 12 treatments.

Treatment	Initial light transmission (%) Mean ± S.D.
1	46.20 ± 5.53
2	4.31 ± 0.58
3	6.811 ± 1.10
4	53.13 ± 3.64
5	0.38 ± 0.34
6	0.27 ± 0.19
7	4.73 ± 0.66
8	3.70 ± 0.45
9	0.27 ± 0.18
10	3.41 ± 1.15
11	87.52 ± 3.59
12	4.32 ± 1.00

Table 3
Analysis of variance (ANOVA) of the RSM models.

RSM models	Source	DF	Sum of squares	Mean square	F ratio	*p*-value
% Light transmission, $R^2 = 0.9906$	Model	6	8810.9	1468.5	87.5	<0.0001*
	Error	5	83.9	16.8		
	Total	11	8894.8			
TS_o, $R^2 = 0.9375$	Model	6	17.809	2.968	12.51	0.0070*
	Error	5	1.187	0.2374		
	Total	11	18.996			
Final gel fraction, $R^2 = 0.8574$	Model	6	0.1399	0.02331	5.011	0.0488*
	Error	5	0.0233	0.00465		
	Total	11	0.1632			
M_n reduction sensitivity (b), $R^2 = 0.8842$	Model	6	1.023e-4	0.000017	6.37	0.0302*
	Error	5	1.339e-5	2.679e-6		
	Total	11	1.157e-4			
Gel-forming rate Gel_b, $R^2 = 0.8959$	Model	6	7.058e-5	0.000012	7.17	0.0236*
	Error	5	8.200e-6	1.641e-6		
	Total	11	7.878 e-5			

Note: * indicates a statistical significance at type I error (α) of 0.05.

3.3. Estimated final tensile strength TS_o

From ANOVA (Table 3), an R^2 of 0.9375 and *p*-value of 0.007 indicate that the second-order RSM model can be applied to the estimated final tensile strength. The linear main effect of CB was the only factor that was significant with *p*-value of 0.0004 (Table 4). The positive parameter estimate (of 1.414) indicates that PBAT films with higher concentrations of CB resulted in greater final tensile strength after exposure to UV light.

3.4. Gel fraction

During exposure to UV radiation, the gel fraction of PBAT film samples increased from 0 mg/mg at the beginning of the test to 0.23–0.64 mg/mg (Table 6) due to crosslinking and recombination of free radicals. The patterns of the increase in gel fraction were similar among all 12 treatments. Initially, the gel fraction developed rapidly, but then reached a plateau stage as time proceeded due to limitations of chain flexibility, polymer crystallinity, and/or availability of the free radicals (Fig. 3) [19]. The development of gel fraction as a function of time followed an exponential increase to a maximum.

$$Gel = Gel_a\left(1 - e^{-Gel_b x}\right) \quad (3)$$

was used to fit the gel fraction as a function of UV radiation for each PBAT treatment. The estimated gel fraction of PBAT exposed to x MJ/m^2 of UV radiation (Gel) is a function of the estimated maximum gel fraction of PBAT sample (Gel_a) and gel-forming rate (Gel_b). The Gel_a, Gel_b, and R^2 values are shown in Table 6. The R^2 values in Table 6 indicate that Equation (3) describes well the pattern of gel fraction in the exposed PBAT films since all treatments have R^2 values greater than 0.9180.

Table 4
Parameter estimates of RSM models for initial light transmission, estimated final tensile strength TS_o, final gel fraction, and M_n reduction sensitivity b from $M_n = y_o + ae^{bx}$.

RSM models	Term	Estimate	*p*-value
Initial light transmission	Intercept	4.89	0.0627
	CB_C	−27.76	<0.0001*
	$AnOx_C$	−1.01	0.5150
	$CB_C \times AnOx_C$	1.76	0.4289
	$CB_C \times CB_C$	19.78	<0.0001*
	$AnOx_C \times AnOx_C$	−0.232	0.8917
	Block	0.597	0.6354
TS_o	Intercept	6.31	<0.0001*
	CB_C	1.414	0.0004*
	$AnOx_C$	0.375	0.0813
	$CB_C \times AnOx_C$	0.1161	0.6538
	$CB_C \times CB_C$	−0.0657	0.7470
	$AnOx_C \times AnOx_C$	0.234	0.2790
	Block	0.127	0.4068
Final gel fraction	Intercept	0.326	0.0002*
	CB_C	−0.108	0.0066*
	$AnOx_C$	−0.00039	0.9877
	$CB_C \times AnOx_C$	−0.0273	0.4598
	$CB_C \times CB_C$	0.0702	0.0481*
	$AnOx_C \times AnOx_C$	0.0169	0.5588
	Block	−0.0325	0.1593
M_n reduction sensitivity (b)	Intercept	−0.00166	0.0983
	CB_C	0.00311	0.0030*
	$AnOx_C$	0.00106	0.1269
	$CB_C \times AnOx_C$	−0.00054	0.5385
	$CB_C \times CB_C$	−0.00091	0.2186
	$AnOx_C \times AnOx_C$	0.00072	0.3164
	Block	0.00059	0.2670

Note: * indicates statistical significance at type I error (α) of 0.05. CB_C and $AnOx_C$ are the coded concentration of carbon black and antioxidants, respectively.

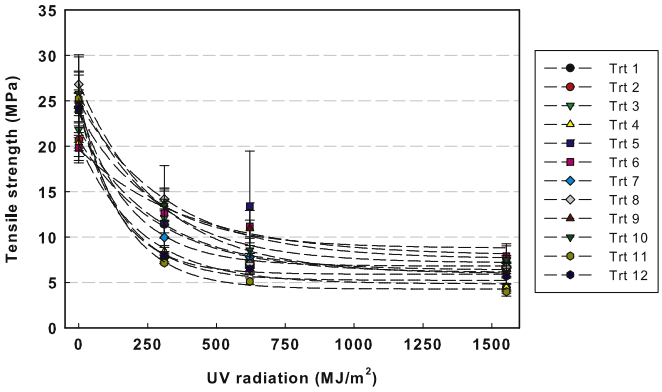

Fig. 2. Changes of tensile strength of all 12 PBAT film treatments as a function of UV radiation in MJ/m^2; dashed lines represent non-linear first order reduction $TS = TS_o + TS_a e^{-TS_b x}$ trend lines.

3.5. Gel_b parameter

A *p*-value of 0.0236 and R^2 value of 0.8959 indicate that the second-order RSM can be applied to the Gel_b parameter (Table 3). From the parameter estimates of the RSM model in Table 7, both linear and quadratic main effects of the coded level of CB affected the Gel_b parameter with *p*-values of 0.0064 and 0.0485. The positive estimate for CB_C indicates that a greater CB concentration will result in greater gel-forming rates. This can be seen from Fig. 3, where PBAT treatments with higher amounts of CB concentrations

Table 5
TS_o, TS_a, and TS_b fitted parameters of non-linear first order reduction of tensile strength of all 12 treatments and their R^2 value.

Treatment	TS_o (MPa)	TS_a (MPa)	TS_b (m^2/MJ)	R^2
1	5.24	19.05	0.0062	0.9780
2	6.09	14.64	0.0034	0.9943
3	6.37	15.57	0.0036	0.9569
4	4.86	15.47	0.0045	0.9862
5	8.79	14.90	0.0038	0.8923
6	7.94	11.74	0.0025	0.9560
7	6.82	17.51	0.0054	0.9964
8	5.96	21.01	0.0034	0.9624
9	7.60	17.27	0.0031	0.9802
10	7.17	18.68	0.0037	0.9934
11	4.30	20.96	0.0063	0.9973
12	5.92	18.24	0.0069	0.9978

Table 6
Final gel fraction, Gel_a and Gel_b fitted parameters of $Gel = Gel_a(1 - e^{-Gel_b x})$ for gel fraction of all 12 treatments and their R^2 value.

Treatment	Final gel fraction[a] (mg/mg) Mean ± S.D.	Gel_a (mg/mg)	Gel_b (10^{-3} m^2/MJ)	R^2
1	0.591 ± 0.034	0.586	2.74	0.9913
2	0.316 ± 0.036	0.358	4.36	0.9997
3	0.297 ± 0.079	0.491	1.89	0.9528
4	0.416 ± 0.116	0.432	3.08	0.9849
5	0.268 ± 0.006	0.280	10.30	0.9942
6	0.228 ± 0.028	0.319	3.06	0.9180
7	0.346 ± 0.035	0.392	2.97	0.9923
8	0.331 ± 0.026	0.341	4.24	0.9936
9	0.378 ± 0.011	0.369	8.71	0.9968
10	0.334 ± 0.027	0.366	3.12	0.9855
11	0.640 ± 0.001	0.670	2.51	0.9752
12	0.471 ± 0.015	0.516	1.78	0.9471

[a] Only mean values from three replicates were used in the RSM calculation.

developed gel more quickly than those with lower concentrations in the initial phase. Later the treatments with higher concentrations reached the plateau stage faster at a lower amount of gel fraction. In addition, there was a significant interaction term of $CB_C \times AnOx_C$ with the estimated parameter of 0.00190 and p-value of 0.0315. Although the purpose of incorporating CB or BHT into the polymer is to protect the polymer from degradation, increased concentration of CB and BHT seems to increase the gel-forming rate, which is an antagonistic effect. Kovács and Wolkober (1976) reported that the mutual effect of CB and phenolic antioxidants, such as BHT, on photooxidation is usually antagonistic due to the reaction of the C═O functional group on the CB surface, which is a stronger hydrogen acceptor than a chain propagating free radical, and the −OH functional group on the phenolic antioxidants leading to lower amounts of BHT with antioxidant capability, with a few cases of synergism [20]. FTIR spectra in Fig. 4 confirm that there is higher absorbance in the carbonyl group (1710 cm^{-1}) of PBAT with CB than that of neat PBAT resin, which might contribute to the antagonistic effect between CB and BHT.

3.6. Final gel fraction

The increased gel fraction resulted in lower biodegradability of the PBAT film [7]. Percent mineralization of the films with gel fraction of 0.10, 0.30, 0.50, and 0.70 mg/mg was 36, 43, 21, and 24%, respectively, during the 45-day test under composting environments [7]. Therefore, the actual final gel fractions of all 12 treatments were used in the RSM model. The second-order RSM model is applicable to the final gel fraction data with p-value of 0.0488 and

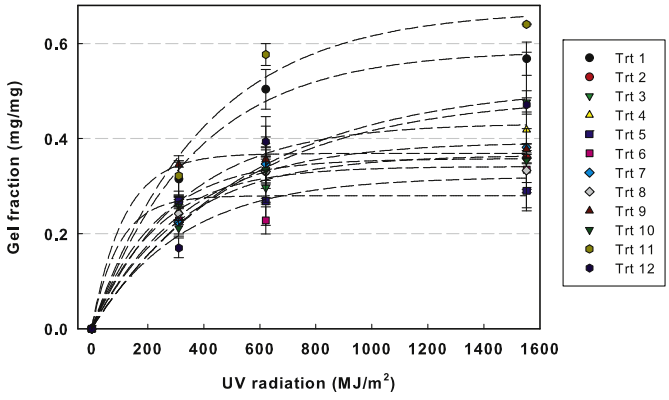

Fig. 3. Changes of gel fractions of all 12 PBAT film treatments as a function of UV radiation in MJ/m^2; dashed lines represent $Gel = Gel_a(1 - e^{-Gel_b x})$ trend lines.

Table 7
Parameter estimates of response surface methodology (RSM) model for gel-forming rate (Gel_b) parameter.

Term	Estimate	p-value
Intercept	0.00336	0.0033*
CB_C	0.00204	0.0064*
$AnOx_C$	0.00110	0.0598
$CB_C \times AnOx_C$	0.00190	0.0315*
$CB_C \times CB_C$	0.00131	0.0485*
$AnOx_C \times AnOx_C$	−0.000265	0.6226
Block	0.000176	0.6544

Note: * indicates a statistical significance at type I error (α) of 0.05. CB_C and $AnOx_C$ are the coded concentration of carbon black and antioxidants, respectively.

R^2 of 0.8574 (Table 3). From the parameter estimates of the RSM model in Table 4, only linear and quadratic main effects significantly affected the final gel fractions of the PBAT treatments. The negative estimated parameter for CB_C of −0.108 indicates that greater CB concentration will result in lower gel development. The UV absorbing ability of CB may contribute to this finding since greater CB concentration results in less photon energy to interact with polymer chains.

3.7. Number average molecular weight

As the PBAT films were exposed to UV radiation, the M_n of treatments decreased differently (Fig. 5). Therefore, it was challenging to find a single equation to represent the reduction pattern for all the treatments. Therefore, a non-linear exponential equation:

$$M_n = y_o + ae^{bx} \quad (4)$$

was selected since this equation can define a variety of reduction patterns (Fig. 6). Here, M_n,— the number average molecular weight of PBAT film exposed to x MJ/m^2 of UV radiation, is defined by three adjusted parameters y_o, a and b, where $y_o + a$ equals the initial M_n at $x = 0$ MJ/m^2 and b is the reduction rate.

With this equation, there are three possible cases of M_n reduction (Fig. 6):

1. In the case $b = 0$; there are no changes in M_n.
2. In the case $a > 0$, $b < 0$; this is a first order exponential reduction, similar to M_n reduction in bulk erosion during

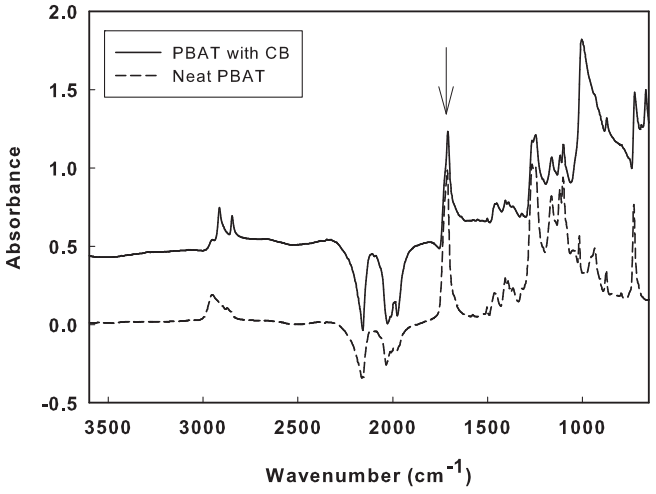

Fig. 4. FTIR spectra of PBAT with carbon black (CB) and neat PBAT resins. The arrow at 1710 cm^{-1} indicates the higher absorbance carbonyl groups of PBAT with CB than that of neat PBAT resin.

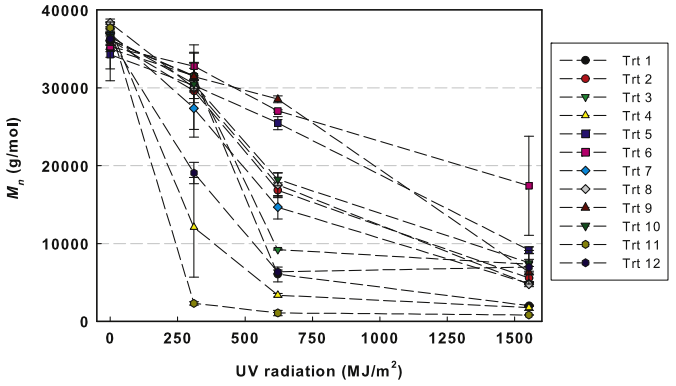

Fig. 5. Reduction of M_n of all 12 treatments of PBAT films as function of time.

biodegradation [21], where there is a rapid reduction in the initial phase and then the reduction reaches the plateau stage.

3. In the case $a < 0$, $b > 0$; M_n decreases slowly at first and then the reduction becomes greater as the films are exposed to more radiation. This reduction pattern is similar to surface erosion of biodegradation [21].

Equation (4) was used to fit the M_n reduction patterns of all 12 PBAT treatments, and the fitted parameters, R^2, and adjusted R^2 are presented in Table 8. Table 8 shows that the equation $M_n = y_o + ae^{bx}$ represents the M_n reduction pattern well, since R^2 values are at least 0.79 and higher and the adjusted R^2 values are close to the R^2 values, which indicates that all three parameters (y_o, a, and b) are explanatory variables for M_n and none are redundant in describing the model [22]. There are only 4 treatments (5, 6, 9, and 10) that have a positive b parameter. Those treatments have CB concentrations of 0.82 or greater, except treatment 10, as has 0.39% CB and 1% BHT.

3.8. M_n reduction sensitivity or parameter b

It is important to use the b parameter, named M_n reduction sensitivity, in the RSM model, since it is indicative of the M_n reduction rate of the PBAT films due to UV exposure. The R^2 value of 0.8842 and p-value of 0.0302 also indicates that the second-order RSM model is applicable to the M_n reduction sensitivity from all

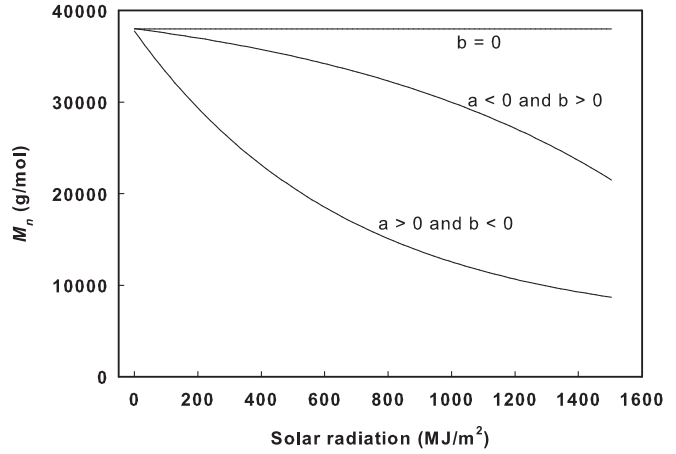

Fig. 6. Schematic reduction pattern of $M_n = y_o + ae^{bx}$ equation with different a and b parameters; for $a < 0$ and $b > 0$ ($y_o = 42.5 \times 10^3$ g/mol, $a = -4.5 \times 10^3$ g/mol and $b = 0.001$ m^2/MJ), and for $a > 0$ and $b < 0$ ($y_o = 5.2 \times 10^3$ g/mol, $a = 32.5 \times 10^3$ g/mol and $b = -0.0015$ m^2/MJ).

Table 8
Fitted y_o, a, and b parameters, R^2, and adjusted R^2 from for M_n reduction of all 12 PBAT treatments.

Treatment	y_o (10^3 g/mol)	a (10^3 g/mol)	b (10^{-3} m^2/MJ)[a]	R^2	Adjusted R^2
1	1.93	35.86	−1.84	0.8174	0.7992
2	5.24	32.51	−1.49	0.9087	0.8996
3	6.11	32.14	−1.91	0.8316	0.8148
4	1.47	36.28	−4.12	0.9660	0.9626
5	36.82	−4.66	1.15	0.9496	0.9445
6	37.52	−4.17	1.03	0.7926	0.7719
7	4.73	33.36	−1.72	0.9588	0.9547
8	4.57	35.27	−1.52	0.9595	0.9555
9	36.69	−2.83	1.53	0.9833	0.9817
10	37.14	−6.33	1.02	0.8247	0.8072
11	0.79	36.92	−10.3	0.9995	0.9995
12	5.50	31.17	−3.27	0.9627	0.9590

[a] Parameter b was named as "M_n reduction sensitivity".

of the treatments (Table 3). The parameter estimates show that only the linear main effect of coded concentration of CB is significant with the estimate of 0.0031 (Table 4), indicating that greater CB concentration will result in an increased M_n reduction sensitivity, which was previously observed.

3.9. Overlaid RSM models

It can be seen from the ANOVA (Table 3) that the second-order RSM models can be applied to all of the four parameters: initial light transmission, estimated final tensile strength, final gel fractions, and M_n reduction sensitivity. In order to determine the optimal concentrations of CB and BHT, it is critical to determine the required criteria for the mulch films first. The criteria for light transmission, tensile strength, and gel fractions were determined based on the authors' previous tomato production trial [23]. For light transmission, films with light transmission in the PAR range of 20% or less can provide the same weed control level as LDPE mulch film [23,24]. For the final tensile strength, the black PBAT film provided adequate weed suppression throughout the whole season and the marketable yields from the plots using this film were comparable to those from the plots using conventional PE mulch film. The tensile strength of the black PBAT film when it started to disintegrate was 6.35 MPa [3]. For the gel fraction, it was expected that after UV exposure, among all of the 12 treatments, PBAT films without any gel could not be achieved. In the authors' previous study, the % biodegradation of PBAT films with gel fractions of 0.10 and 0.30 mg/mg in manure composting environments for 45 days were 36 and 43%, respectively, and they were not statistically different [7]. Therefore, gel fraction of 0.30 mg/mg was selected as the target criterion.

In this experiment, treatments 5, 6, 9, and 10 are the only four treatments with positive M_n reduction sensitivity. The treatments with $b > 0$ were the four treatments with the lowest % light transmission (Table 2), the highest final tensile strength (Table 5), and relatively low final gel fraction of less than 0.38 mg/mg(Table 6). In the case of negative M_n reduction sensitivity ($b < 0$), the rapid reduction of M_n at first along with the damage from wind and animals in the field means the films will not last long. On the other hand, in the case of positive M_n reduction sensitivity ($b > 0$), the film will last longer in the field since initially the film can better retain its properties and then rapidly degrade right before or after the harvest. This is desirable in vegetable production where retention of properties early in the season is more important than later. Therefore, M_n reduction sensitivity was selected as an input variable for the RSM model since the molecular weight reduction where positive M_n reduction sensitivity $b \geq 0$ is more desirable.

Therefore, four response surface models were analyzed simultaneously. Those selected four models and their criteria are light

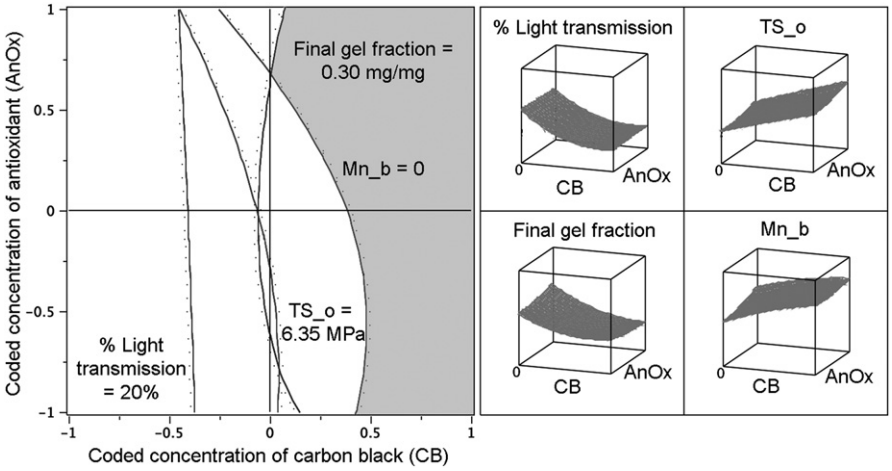

Fig. 7. The overlaid contour plot of the four response surface models: % light transmission, final tensile strength, final gel fraction, and M_n reduction sensitivity (*Mn_b*). The shaded area is the intersection where the criteria of all four models are fulfilled.

transmission of 20% or less, final tensile strength of at least 6.35 MPa, final gel fraction of less than 0.30 mg/mg, and M_n reduction sensitivity $b \geq 0$. These criteria are subjective and can be changed depending on the solar radiation and length of the crop production season.

By using those criteria in the four RSM models shown in Table 4, the overlaid contour plot of all four RSM models was obtained. The shaded area in the overlaid contour plot (Fig. 7) is the intersection where all the four criteria are met or exceeded. Any combination of CB and BHT concentrations in this area should be suitable for PBAT mulch films for tomato production (3–4 months of UV exposure) in Michigan or regions with similar or lower solar radiation during the growing season from May to September (shaded region in Fig. 8), which have an average monthly solar radiation of 7.2–21.6 MJ/m^2/d.

3.10. Effect of antioxidant

The overlaid contour plot (Fig. 7) suggests that incorporation of a high amount of BHT (higher than 0.67% or coded level of 0.5) allows CB to be used at a lower concentration. CB concentration of 0.59% (coded level of 0.5) can be used when BHT concentration is greater than 0.5% (coded level of 0). This is desirable since an increased amount of CB may hinder film production.

BHT has slight effects on tensile strength and M_n reduction sensitivity. Besides treatments 1, 4, and 11, where CB concentrations were 0.1, 0.1, and 0%, respectively, treatment 12 with 0% BHT and 0.39% CB yields the lowest final tensile strength (Table 5), the lowest M_n reduction sensitivity (Table 8) and the highest gel fraction at the end of the test (Table 6) among the treatments with 0.39% CB or higher. Furthermore, treatment 10, which has 0.39% CB and the highest BHT concentration of 1.0% among all the treatments, shows the highest final tensile strength (Table 5) and lowest M_n reduction among the treatments with 0.39% CB (second only to the treatments with 0.82% CB). Treatment 10 is also the only treatment with 0.39% CB that has a positive M_n reduction sensitivity.

From the parameter estimates from the four response models (initial light transmission, estimated final tensile strength, final gel fraction, and M_n reduction sensitivity), CB concentration was the main treatment resulting in improved film photo-stability, while the main effect of antioxidant was not significant. It is not that BHT does not have an effect on tensile strength and M_n reduction sensitivity, but the effect is overwhelmed by influence of CB. In addition, the antagonistic effect of CB and BHT was observed in the gel-forming rate.

Fig. 8. The area in the U.S. where the film formulation in Fig. 7 can be used as mulch film for 3–4 month field production. The shaded areas are the areas with similar or lower average solar radiation to Michigan. Source: National Renewable Energy Laboratory: Resource Assessment Program [25].

4. Conclusions

The response surface methodology presented in this paper can be used as guidance in selecting appropriate concentrations of carbon black and antioxidant for mulch film application of PBAT film based on optimization of multiple performance parameters at the same time using fitted equations and simultaneous RSM analysis. In this case, suitable compositions of carbon black and antioxidant for the PBAT mulch films used in Michigan or regions with similar climate were determined by intersecting the concentrations of carbon black and BHT producing films that exceed all four required criteria of light transmission (20% or less), final tensile strength (of at least 6.35 MPa), gel fraction (<0.30 mg/mg), and M_n reduction sensitivity larger than zero. As assumed, the second-order RSM is enough to capture the essence of the response surface from actual experimental data of initial light transmission, estimated final tensile strength, final gel fraction, and M_n reduction sensitivity with R^2 of 0.85 or higher without sacrificing degree of freedom. Although this experiment is based on PBAT with 40% aromatic content and used for mulch film application, the same

methodology can be applied to PBAT with different aromatic content, different plastics, and other applications, such as greenhouse films and plastic pots. However, further experiments need to be conducted in order to obtain the required data for these models.

Besides all the advantages, there are some limitations of the current model due to the specific testing conditions and boundary conditions of the preselected carbon black and antioxidant concentrations. First, from Fig. 7, the carbon black concentration with best performance seems to be outside of the RSM boundary. Therefore, the boundary of a future recommended RSM study should be shifted toward higher carbon black concentrations, such as from 0.4 to 2% carbon black by mass (instead of 0–1%). Second, due to the limitation of the instrument, only the chain breaking antioxidant was included in this experiment. In order to completely study the synergistic and antagonistic effect of antioxidants on PBAT mulch films, the use of peroxide decomposing antioxidant should be investigated. Third, this model is not applicable in the case where the second-order response surface equations cannot represent the data, *e.g.*, initial light transmission, estimated final tensile strength, final gel fraction, and M_n reduction sensitivity, from all of the treatments. Finally, for the PBAT film used during the summer growing season in Michigan or area with similar climate or similar solar radiation (7.2–21.6 MJ/m^2/d) or lower, this model can be applied directly. However, it is not recommended to use this model for other regions, different plastics, or different exposure duration. In order to expand the model to represent other U.S. regions, the length of the UV radiation test has to be extended, such as 21.6–36 MJ/m^2/d for the Southwest [25]. Consequently, an RSM model for general radiation can be developed by including the total solar radiation into the model as another variable, besides carbon black and antioxidant concentrations.

Acknowledgments

Authors would like to thank the Michigan Agricultural Experiment Station for funding the two-year preliminary tomato production trials through project GREEEN of grant numbers GR05-020D and GR06-089, Northern Technologies International Inc. for providing PBAT master batch.

References

[1] Schnabel W. Polymer degradation: principles and practical applications. New York: Hanser; 1992.
[2] Albertsson AC. Biodegradation of polymers. In: Hamid SH, Amin MB, Maadhah AG, editors. Handbook of polymer degradation. New York: Marcel Dekker; 1992. p. 345–63.
[3] Kijchavengkul T, Auras R, Rubino M, Ngouajio M, Fernandez RT. Assessment of aliphatic–aromatic copolyester biodegradable mulch films. Part I: field study. Chemosphere 2008;71:942–53.
[4] Rivaton A, Gardette JL. Photo-oxidation of aromatic polymers. Angew Makromol Chem 1998;261/262:173–88.
[5] Tabankia M, Gardette JL. Photo-chemical degradation of polybutylene terephthalate: part 1-photo-oxidation and photolysis at long wavelengths. Polym Degrad Stabil 1986;14:351–65.
[6] Valk VG, Kehren ML, Daamen I. Photooxidation of poly(ethyleneglycol terephthalate). Angew Makromol Chem 1970;13:97–107.
[7] Kijchavengkul T, Auras R, Rubino M, Ngouajio M, Fernandez RT. Assessment of aliphatic–aromatic copolyester biodegradable mulch films. Part II: laboratory simulated conditions. Chemosphere 2008;71:1607–16.
[8] Kijchavengkul T, Auras R, Rubino M, Selke S, Ngouajio M, Fernandez RT. Biodegradation and hydrolysis rate of aliphatic aromatic polyester. Polym Degrad Stabil 2010;95:2641–7.
[9] Witt U, Einig T, Yamamoto M, Kleeberg I, Deckwer WD, Muller RJ. Biodegradation of aliphatic–aromatic copolyesters: evaluation of the final biodegradability and ecotoxicological impact of degradation intermediates. Chemosphere 2001;44:289–99.
[10] Lamont W. Plastic mulches. In: Lamont W, editor. Production of vegetables, strawberries, and cut flowers using plasticulture. Ithaca: Natural Resource, Agriculture, and Engineering Service (NRAES); 2004. p. 9–14.
[11] Shlyapintokh V. Photochemical conversion and stabilization of polymers. New York: Hanser; 1984.
[12] Myers R, Montgomery D, Anderxon-Cook C. Response surface methodology: process and product optimization using designed experiments. Hoboken, NJ: John Wiley & Sons; 2009.
[13] ASTM D6400-04 standard specification for compostable plastics. West Conshohocken, PA: ASTM International; 2004.
[14] Kijchavengkul T, Auras R, Rubino M, Alvarado E, Camacho Montero JR, Rosales JM. Atmospheric and soil degradation of aliphatic–aromatic polyester films. Polym Degrad Stabil 2010;95:99–107.
[15] Ngouajio M, Ernest J. Light transmission through colored polyethylene mulches affects weed populations. Hortscience 2004;39:1302–4.
[16] ASTM D882-98 standard test method for tensile properties of thin plastic sheeting. West Conshohocken, PA: ASTM International; 1998.
[17] ASTM D2765-01 standard test methods for determination of gel content and swell ratio of crosslinked ethylene plastics. West Conshohocken, PA: ASTM International; 2006.
[18] Kijchavengkul T, Auras R, Rubino M. Measuring gel content of aromatic polyesters using FTIR spectrophotometry and DSC. Polym Test 2008;27:55–60.
[19] Jia Zhen S. The effect of chain flexibility and chain mobility on radiation crosslinking of polymers. Radiat Phys Chem 2001;60:445–51.
[20] Kovács E, Wolkober Z. The effect of the chemical and physical properties of carbon black on the thermal and photooxidation of polyethylene. J Polym Sci Pol Sym 1976;57:171–80.
[21] Kijchavengkul T, Auras R. Perspective: compostability of polymers. Polym Int 2008;57:793–804.
[22] Kutner M, Nachtsheim C, Neter J, Li W. Applied linear statistical model. 4th ed. New York: McGraw-Hill /Irwin; 2004.
[23] Ngouajio M, Auras R, Fernandez RT, Rubino M, Counts JW, Kijchavengkul T. Field performance of aliphatic–aromatic copolyester biodegradable mulch films in a fresh market tomato production system. Horttechnology 2008;18:605–10.
[24] Kijchavengkul T. Design of biodegradable aliphatic aromatic polyester films for agricultural applications using response surface methodology. School of packaging, Doctoral dissertation. East Lansing, MI: Michigan State University, 2010.
[25] U.S. Solar Radiation Resource Maps. Washington, D.C.: National renewable energy laboratory: resource assessment program. 1994 (accessed 13.08.10), Available from: http://rredc.nrel.gov/solar/old_data/nsrdb/redbook/atlas/.